

Star formation in damped Ly α systems

Arthur M. Wolfe

CASS, University of California, San Diego, La Jolla, CA 92093-0424, USA
email: awolfe@ucsd.edu

Abstract. We determine star formation rates for a sample of 50 DLAs from properties of the absorbing gas alone. Assuming thermal balance, we determine the grain photoelectric heating rate of the neutral gas from the [C II] 158 μm cooling rate per H atom, ℓ_c , inferred from C II* 1335.7 and damped Ly α absorption lines. We deduce the star formation rate per unit area and the FUV luminosity per unit co-moving volume, \mathcal{L}_ν^{DLA} . Comparison of \mathcal{L}_ν^{DLA} with the luminosity density of Lyman Break Galaxies, \mathcal{L}_ν^{LBG} , shows that $\mathcal{L}_\nu^{DLA} \gg \mathcal{L}_\nu^{LBG}$ for most models. These models are ruled out if our assumption that LBGs dominate the total FUV luminosity density of the Universe is correct. The only feasible models are those in which $\mathcal{L}_\nu^{DLA} \approx \mathcal{L}_\nu^{LBG}$. We conclude that DLAs in which $\ell_c > 10^{-27.1} \text{ ergs s}^{-1} \text{ H}^{-1}$ contain centrally located LBGs, while the gas in DLAs with $\ell_c < 10^{-27.1} \text{ ergs s}^{-1} \text{ H}^{-1}$ is heated by background radiation alone.

1. Introduction

Damped Ly α systems (DLAs) are QSO absorption systems defined to have H I column densities, $N(\text{H I}) > 2 \times 10^{20} \text{ cm}^{-2}$. This threshold assures that gas in DLAs is predominantly neutral at high redshifts because gas layers with lower H I column densities become ionised (Viegas 1995; Prochaska & Wolfe 1996) when subjected to the high intensity of ionising non-thermal background radiation in the redshift interval $z=[2,5]$ (Haardt & Madau 2004). Because clouds of neutral atomic gas are the progenitors of molecular clouds (Wolfire *et al.* 2003) and molecular clouds are the sites of star formation in The Galaxy, star formation is more likely to be associated with DLAs than with the ionised gas comprising all other classes of absorption systems.

The neutrality of the gas takes on added significance when it is realised that DLAs (1) dominate the neutral gas content of the Universe in the redshift interval $z=[0,5]$ and (2) contain sufficient gas at $z=[3,4]$ to account for about half the visible baryons in modern galaxies (see Wolfe, Gawiser & Prochaska 2005 [WGP05]). This has led to the widely accepted idea that DLAs serve as important reservoirs of neutral gas for star formation at high redshifts (e.g. Nagamine *et al.* 2004). While such reservoirs can supply gas for star formation, they can also be replenished by gas infall from the IGM. Consequently, the co-moving mass density of neutral gas $\Omega_{gas}(z)$ need not exceed the current co-moving mass density of stars $\Omega_*(0)$ to qualify as a neutral gas reservoir for star formation.

While the near equality of $\Omega_{gas}(z=2 \rightarrow 3)$ and $\Omega_*(0)$ suggests that DLAs supply the “fuel” for star formation at high redshifts, other independent evidence is needed before this idea can be taken seriously. Direct detection of starlight from galaxies associated with the absorbing gas is of course unambiguous evidence for star formation. The evidence is clear at low redshifts because galaxies of stars have been detected in about half of the known sample of 23 DLAs with $z < 1$ (Chen *et al.* 2005; WGP05). On the other hand, Table 1 shows that meaningful constraints on star formation rates (SFRs) have been established for only five legitimate DLAs with $z > 1.7$. The SFR for DLA2206–19A is comparable to the median SFR of the spectroscopic sample of Lyman Break Galaxies (LBGs), i.e. LBGs brighter than $R_{AB}=25$. By contrast, the SFRs for the two objects

Table 1. SFRs inferred from DLA emission

DLA	Redshift	Method	SFR ($M_{\odot} \text{ yr}^{-1}$)	Ref.
0458–02	2.040	Ly α	> 1.5	Møller <i>et al.</i> 2004
0953+47	3.407	Ly α	0.7→ 7.0	Bunker <i>et al.</i> 2004
2206–19A	1.921	Broad-band	25→ 50	Møller <i>et al.</i> 2002
1210+17	1.892	H α	< 5.0	Kulkarni <i>et al.</i> 2001
1244+34	1.892	H α	< 1.6	Kulkarni <i>et al.</i> 2000

with upper limits are less than the SFRs of LBGs at the faint end of the LBG luminosity function, which goes to $R=27$ (Steidel *et al.* 1999). Therefore, while the SFRs for a few high redshift DLAs are at the high and low extremes of the SFR distribution of LBGs, the distribution of SFRs for a fair sample of DLAs is currently unknown.

For these reasons my colleagues and I have been working on a technique to fill in this gap, a technique which does not depend on flux-limited samples galaxies, but rather depends on properties of the absorbing gas alone. In this contribution, I briefly describe the physics behind this technique in § 2, describe how global constraints discriminate among various models in § 3, and describe the relationship between DLAs and LBGs that emerge from these considerations in § 4.

2. CII* technique for measuring star formation in DLAs

2.1. ISM fundamentals

The idea (discussed in Wolfe, Prochaska & Gawiser 2003 [WPG03]; Wolfe, Gawiser & Prochaska 2003 [WGP03]; Wolfe *et al.* 2004 [WHGPL04]) is that massive stars forming in DLAs emit FUV radiation (photon energies $h\nu=6$ to 13.6 eV) that heats the gas through grain photoelectric heating (see Wolfire *et al.* 2003). The heating rate $\Gamma_{pe}=10^{-5}\kappa\epsilon J_{\nu}$ ergs $s^{-1}H^{-1}$ where J_{ν} is the FUV mean intensity, ϵ is the heating efficiency, and κ is the dust-to-gas ratio. The crucial point is that J_{ν} is proportional to the luminosity per unit H I area, L_{ν}/A_{HI} , which in the case of FUV radiation is proportional to the instantaneous SFR per unit H I area, $\dot{\psi}_{*}$. Several authors have computed ϵ and show it to depend on the parameter $J_{\nu}\sqrt{T}/n_e$ where T and n_e are gas temperature and electron density (e.g. Weingartner & Draine 2001; Bakes & Tielens 1994). Because κ can be computed from depletion patterns in the absorbing gas (WPG03), we can determine $\dot{\psi}_{*}$ from the heating rate provided the thermal phase of the DLA gas is specified.

WPG03 measured the heating rate by equating it to the cooling rate; i.e. they assumed thermal balance. In the Galaxy ISM cooling is dominated by [C II] 158 μm emission, which is produced by spontaneous emission between the excited $^2P_{3/2}$ and ground $^2P_{1/2}$ states in the $2s^22p$ term of C^+ . This emission rate can be inferred from UV spectroscopy by measurements of the C II* 1335.7 absorption line which arises from transitions between the $^2P_{3/2}$ and higher lying $^2D_{3/2}$ and $^2D_{5/2}$ states. WPG03 estimate the [C II] 158 μm cooling rate per H atom from the quantity $\ell_c\equiv N(C \text{ II}^*)h\nu_{ul}A_{ul}/N(H \text{ I})$ (ergs $s^{-1}H^{-1}$), where $N(C \text{ II}^*)$ is the measured C II* column density, and $h\nu_{ul}$ and A_{ul} are the energy and Einstein A coefficient of the 158 μm transition.

2.2. Application to DLAs

WHGPL04 recently published measurements of ℓ_c obtained from accurate C II* velocity profiles obtained with the HIRES and ESI spectrographs on the Keck 10 m telescopes. From a sample of 52 DLAs they found positive detections for about half the sample and upper limits for the remaining half. The results in Fig. 1 indicate that the median for the

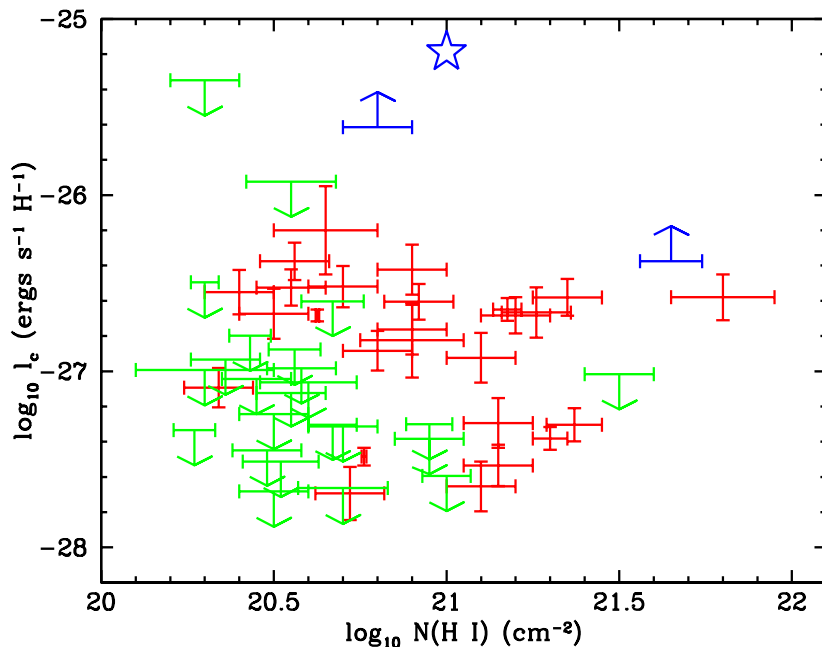


Figure 1. ℓ_c versus $N(\text{H I})$ for sample of 52 DLAs. Red, green, blue data points are positive detections and 95 % confidence upper limits and lower limits. The star is the value of ℓ_c obtained for The Galaxy disk from COBE measurements of $[\text{C II}] 158 \mu\text{m}$ emission (Wright *et al.* 1991).

positive detections, $\ell_c = 10^{-26.6}$ ergs $\text{s}^{-1} \text{H}^{-1}$, is about a factor of 30 below the average for The Galaxy. Since this also equals the ratio of κ for DLAs to the Galaxy ISM, WPG03 assumed the lower cooling (i.e. heating) rates in DLAs were due to the lower dust-to-gas ratios in DLAs rather than lower SFRs.

To test this hypothesis WPG03 computed the thermal equilibrium of H I layers in which the heating rate $\Gamma = \Gamma_{pe} + \Gamma_{CR} + \Gamma_{XR} + \Gamma_{C I}$, where Γ_{CR} and Γ_{XR} are heating rates due to ionisation of H by cosmic rays and soft X-rays (both the XR and CR heat inputs are assumed to be proportional to ψ_*), and $\Gamma_{C I}$ is the heating rate due to photoionisation of C^0 . The cooling rate includes fine-structure transitions from major abundant ions, Ly α emission, and radiative recombination of electrons onto grains. WHGPL04 considered whether the heat input due to background radiation alone was sufficient to account for the ℓ_c values observed in the half of the sample with positive detections. The results for one representative DLA are shown in Fig. 2a. which plots the ℓ_c versus n relation predicted for thermal equilibrium (i.e. heating rate equals cooling rate) of gas heated by background radiation alone, where J_ν^{bkd} for $h\nu = 1$ to 1000 eV was kindly supplied by Haardt & Madau (2004). Fig. 2a indicates that for a fixed J_ν^{bkd} , ℓ_c varies with n . Cooling at low n is dominated by Ly α emission rather than $158 \mu\text{m}$ emission and as a result $\ell_c \ll \Gamma$. In this case the gas is a warm neutral medium (WNM) with temperatures $T \sim 8000$ K. At densities between the vertical dot-dashed lines the gas is thermally unstable and cannot remain at the computed equilibrium for more than 1 cooling time. At densities exceeding that of the right vertical line, the gas is a cold neutral medium (CNM) with $T \sim 100$ K: here cooling is dominated by $158 \mu\text{m}$ emission and $\ell_c = \Gamma$. Fig. 2a shows that background heating alone cannot account for the inferred cooling rate.

The inability of background heating to balance the observed $158 \mu\text{m}$ cooling rate holds for all DLAs with positive detections in which $\ell_c > 10^{-27.1}$ ergs $\text{s}^{-1} \text{H}^{-1}$, where the latter

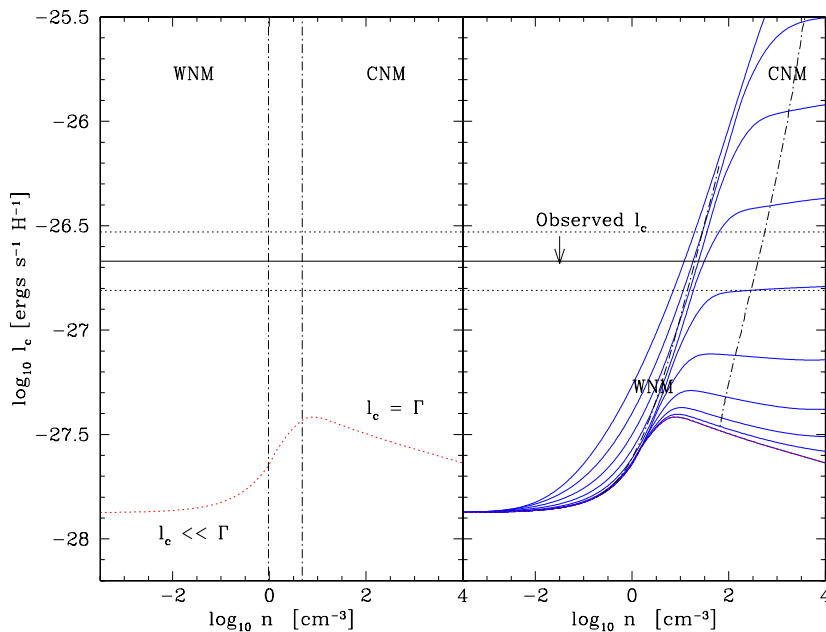


Figure 2. (a) ℓ_c versus gas density n predicted for thermal equilibrium when the gas is heated by background radiation alone. The results are shown for DLA0747+27, a DLA with $z=3.900$ and $N(\text{H I})=10^{20.5} \text{ cm}^{-2}$ (WHGPL04). The horizontal lines correspond to the measurements and 1σ errors. Other notations explained in text. (b) Same as (a) except solid curves correspond to added heat inputs due to local sources with $\log_{10}\dot{\psi}_* = -4.0, -3.5, \dots, 0.0 \text{ M}_\odot \text{ yr}^{-1} \text{ kpc}^{-2}$. Steeply rising dot-dashed lines denote thermally stable CNM and WNM solutions (see text).

is slightly higher than the peak of the ℓ_c versus n relation for background heating alone (see WHGPL04). To achieve thermal balance, local heat sources are required and WHGPL04 suggested that radiative feedback from stars in the local DLA heat the gas. The results of increasing $\dot{\psi}_*$ are shown in Fig. 2b. To choose between the various solutions, WPG03 adopted an analogy with the Galaxy ISM, where the narrow range in gas pressures indicate a two-phase medium in which CNM gas is in pressure equilibrium with WNM gas (Wolfire *et al.* 2003). In that case, two unique solutions for n result for each value of $\dot{\psi}_*$. These are shown as the steeply rising dot-dashed curves in Fig. 2b. The intersection between these curves and the observed ℓ_c specifies $\dot{\psi}_*$. Fig. 2b shows that $\dot{\psi}_*=10^{-1.70}$ and $10^{-0.65} \text{ M}_\odot \text{ yr}^{-1} \text{ kpc}^{-2}$ for the CNM and WNM solutions. Similar results hold for the remaining DLAs with positive detections. This leads to two models. The first is the “CNM” model in which the QSO sight-line passes through WNM and CNM gas and the C II* absorption arises in the CNM gas. The second is the “WNM” model in which the QSO sight-line passes through WNM gas alone. The models are distinguished by a large area covering factor of the CNM gas and moderate SFR per unit H I area in the “CNM” model, and a small area covering factor of the CNM gas and large SFR per unit H I area in the “WNM” model.

What about the DLAs with upper limits on ℓ_c ? WHGPL04 show that in most cases the upper limits are less than about 0.2 dex above the peaks in the predicted ℓ_c versus n curves for background heating alone. As a result, the true values likely intersect these curves and do so at low values of n where the gas is a WNM. As a result, DLAs in which $\ell_c < 10^{-27.1} \text{ ergs s}^{-1} \text{ H}^{-1}$ may be WNM gas heated only by background radiation.

However, we cannot rule out the possibility that higher SFRs are present since ℓ_c is relatively insensitive to increases in ψ_* in the WNM, as shown in Fig. 2b.

3. The DLA-LBG connection

3.1. Global constraints

To discriminate among these possibilities we turn to global constraints. Specifically, Giavalisco *et al.* (2004a) recently presented measurements of the FUV co-moving luminosity density for LBGs, \mathcal{L}_ν^{LBG} , at $z = [2, 6]$. The measurements, which combine the results of the GOODS survey and the results of Steidel *et al.* (1999), correspond to AB magnitudes brighter than 27.8 for rest-frame wavelengths of 1500 Å and reach a limiting 3σ surface brightness of ~ 27.2 mag arc-sec $^{-2}$ at $z \approx 3 \rightarrow 4$ (Giavalisco *et al.* 2004b). As a result, only FUV sources with lower surface brightness would have been missed. While the presence of such objects cannot be ruled out, I shall assume that the GOODS survey has detected all the FUV sources in the high- z Universe and they are in the form of LBGs. This luminosity density acts a source function for J_ν^{bkd} through the relationship

$$J_\nu^{bkd}(z_a) = \frac{c}{4\pi} (1 + z_a)^3 \int_{t(z_{start})}^{t(z_a)} \mathcal{L}_\nu^{LBG}(t) dt \quad (3.1)$$

where $t(z_{start})$ is the earliest time at which FUV sources contribute to the background radiation at $t(z_a)$: I assume this corresponds to the redshift z_{start} at which the Lyman limit discontinuity of the galaxy spectra is redshifted into the FUV wavelength of 1500 Å at z_a . It is important to emphasise that the values of \mathcal{L}_ν^{LBG} contributing to the FUV background are those which have *not been corrected for extinction*, since only photons escaping from LBGs contribute to the background.

The value of J_ν^{bkd} influences the resultant luminosity density contributed by DLAs, \mathcal{L}_ν^{DLA} , because the total mean intensity incident on the absorbing gas is given by

$$J_\nu = J_\nu^{bkd} + J_\nu^{local} \quad , \quad (3.2)$$

where

$$J_\nu^{local} \propto \frac{L_\nu}{A_{HI}} \quad , \quad (3.3)$$

and the dimensionless proportionality constant depends on geometry and the details of radiative transfer. The co-moving luminosity density contributed by DLAs is given by

$$\mathcal{L}_\nu^{DLA} = \frac{H_0}{c} < \frac{L_\nu}{A_{HI}} > \frac{dN}{dX} \quad , \quad (3.4)$$

where $< L_\nu/A_{HI} >$ is the luminosity per unit area averaged over the DLA sample and dN/dX is the number of DLAs per unit absorption distance (see WGP05). As a result, L_ν/A_{HI} and thus \mathcal{L}_ν^{DLA} are affected by the value of J_ν^{bkd} and by the efficiency of grain photoelectric heating. High values of J_ν^{bkd} will lower L_ν/A_{HI} for fixed values of J_ν , while high values of ϵ and κ , i.e. grains that are efficient heaters, will lower J_ν for a given ℓ_c , which also lowers the values of L_ν/A_{HI} .

This analysis has the following implication: because I have assumed that the FUV luminosity density is dominated by \mathcal{L}_ν^{LBG} , there are only two possibilities. Either DLAs are a population of objects distinct from LBGs, in which case $\mathcal{L}_\nu^{DLA} \ll \mathcal{L}_\nu^{LBG}$, or the DLA and LBG populations strongly overlap, in which case $\mathcal{L}_\nu^{DLA} \approx \mathcal{L}_\nu^{LBG}$. When we computed these quantities we found instead that $\mathcal{L}_\nu^{DLA} \gg \mathcal{L}_\nu^{LBG}$ for most models. This follows from the high values of J_ν caused by inefficient heating or by low values of

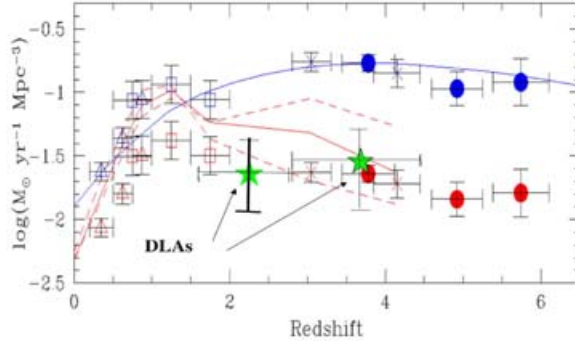


Figure 3. SFR per unit co-moving volume, $\dot{\rho}_*$, versus z from Giavalisco *et al.* (2004a). Note luminosity density \mathcal{L}_ν^{LBG} ($\text{ergs s}^{-1} \text{Hz}^{-1} \text{Mpc}^{-3}$) = $7.1 \times 10^{28} \dot{\rho}_* (\text{M}_\odot \text{yr}^{-1} \text{Mpc}^{-3})$. Red data points are deduced directly from galaxy fluxes while blue data points are rates corrected for extinction. Two stars are predicted co-moving SFR densities for DLAs in the case of maximal heating efficiency.

J_ν^{bkd} . Because of the very large values predicted for J_ν , all the WNM models are excluded (these models also produce excessive bolometric background radiation at $z=0$ [WGP03]). In addition, all CNM models with inefficient heating are excluded, which is a new result. Indeed we found the condition $\mathcal{L}_\nu^{DLA} \ll \mathcal{L}_\nu^{LBG}$ was difficult to achieve even with the most efficient heating by small carbonaceous grains and geometrical conditions that increase the value of J_ν^{local} for a given L_ν/A_{HI} . This conclusion is consistent with Miralda-Escude (2005) who used a similar analysis to place upper limits on the strength of local heat sources in DLAs and other QSO absorbers: our constraints are slightly weaker than his because he used a simplified model of a spherical shell of gas surrounding a point source, while we use a more realistic geometry of an extended gaseous disk surrounding a point source when averaging over all impact parameters to compute $\langle L_\nu/A_{\text{HI}} \rangle$. A typical prediction for our most efficient heating models is shown in Fig. 3.

I conclude that a significant overlap between the DLA and LBG populations is the simplest explanation for these results. In that case, DLAs are exposed to the same FUV radiation field that escapes from LBGs and produces the observed values of \mathcal{L}_ν^{LBG} . As a result, the *intrinsic* values of \mathcal{L}_ν^{DLA} and \mathcal{L}_ν^{LBG} are also equal. In this scenario, FUV radiation emitted by compact centrally located LBGs propagates through and is attenuated by the dust known to be present in LBGs (Shapley *et al.* 2003). The radiation escaping the LBG region then heats the surrounding H I envelope comprising the DLA gas.

Before leaving this topic I briefly comment on the DLAs with $\ell_c < 10^{-27.1} \text{ergs s}^{-1} \text{H}^{-1}$, which comprise about half the objects in our sample. In § 2.2 it is argued that these comprise configurations of WNM gas in which ψ_* is unconstrained. However, the global constraints introduced in this section show that it is crucial to reduce J_ν^{local} in order to bring \mathcal{L}_ν^{DLA} below \mathcal{L}_ν^{LBG} . This is most easily achieved by reducing J_ν^{local} in this subsample of DLAs below J_ν^{bkd} . This also makes physical sense because it is difficult to understand how a high SFR could arise from configurations comprised mainly of WNM gas. Therefore, I suggest that DLAs with $\ell_c < 10^{-27.1} \text{ergs s}^{-1} \text{H}^{-1}$ contain no LBGs, and are thus mainly heated by background radiation. However, it is unlikely that $\psi_* = 0$ since some star formation must be present to account for the heavy element abundances, which are significantly higher than that of the Ly α forest; i.e. chemical enrichment in addition to processes that pollute the IGM are required for these DLAs. As a result, *in situ* SFRs

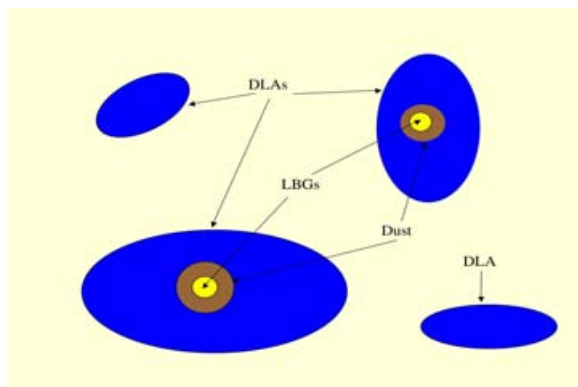


Figure 4. Schematic diagram illustrating relationship between DLAs and LBGs. DLAs with $\ell_c > 10^{-27.1}$ ergs s $^{-1}$ H $^{-1}$ host centrally located LBGs which are sources of FUV radiation that propagates through dust and then heats the surrounding DLA gas. LBGs are absent from DLAs with $\ell_c < 10^{-27.1}$ ergs s $^{-1}$ H $^{-1}$ where the gas is heated mainly by background radiation.

of $\dot{\psi}_* \leq 10^{-4} M_\odot \text{ yr}^{-1} \text{ kpc}^{-2}$ may be present. A schematic diagram summarising these ideas is given in Fig. 4.

3.2. Implications of the DLA/LBG connection

Because high values of \mathcal{L}_ν^{DLA} imply high SFRs per unit co-moving volume, the uniform-disk models of WGP03 predicted high metal enrichment rates throughout the DLA gas. Specifically, WGP03 found that the metals produced exceed the metals observed in DLAs by at least an order of magnitude (see also Nagamine *et al.* 2004). That problem is solved by the present model because primary metal production is confined to the centrally located LBGs, which are known to be metal rich. Metal *enrichment* of the outlying DLA gas does not occur primarily by *in situ* star formation, as in the uniform disk model, but rather may be a by-product of metal-enriched winds coming out of the LBG. These ideas are consistent with the bulge model suggested by WGP03.

Secondly, the *intrinsic* SFR per unit co-moving volume for LBGs is about $0.15 M_\odot \text{ yr}^{-1} \text{ Mpc}^{-3}$ (see Fig. 3). In our model, DLAs would serve as neutral gas reservoirs that transport neutral gas to fuel star formation in the centrally located LBG. Unless replenished by gas inflow from the IGM, the neutral gas reservoirs will be depleted in about 2 Gyr if all DLAs are associated with LBGs. If only those DLAs with $\ell_c > 10^{-27.1}$ ergs s $^{-1}$ H $^{-1}$ harbour LBGs, then the neutral gas reservoirs will be depleted in about 1 Gyr. The implication is that inflow from the IGM into the DLAs is required to sustain the SFRs of the LBGs. Such inflows occur in CDM models for galaxy formation.

3.3. Supporting evidence for the DLA/LBG connection

There are several lines of evidence supporting the connection between DLAs and LBGs (see Schaye 2001). Møller *et al.* (2002) found a bright LBG to be associated with DLA2206–19A as shown in Table 1. Indeed these authors drew attention to the similarity between DLAs and LBGs, but suggested that DLAs would be less massive and hence be less strongly clustered than LBGs. However, Cooke *et al.* (2005) report a strong cross-correlation between DLAs and LBGs. They imaged the fields surrounding QSOs with 11 foreground DLAs with $z \sim 3$. Using multi-colour Lyman “drop-out” techniques, Cooke *et al.* (2005) located over 200 LBGs. A cross-correlation analysis showed that the amplitude of the cross-correlation LBG-DLA function was comparable to the amplitude of

the auto-correlation LBG-LBG function. The implication is that DLAs are biased with respect to mass by the same amount as LBGs (see Bouche & Lowenthal 2003). If confirmed, this tentative detection would imply similar dark-matter masses for DLAs and LBGs, indicating they are drawn from the same populations of objects.

4. Conclusions

We have used the observed FUV luminosity density of the Universe, \mathcal{L}_ν^{LBG} , to constrain the radiation emitted by DLAs. We find that all our previous models with inefficient grain photoelectric heating produce more FUV radiation than observed, i.e. $\mathcal{L}_\nu^{DLA} \gg \mathcal{L}_\nu^{LBG}$, and are therefore unlikely to be correct. The only models consistent with the observations are those in which both the observed and intrinsic values of \mathcal{L}_ν^{DLA} and \mathcal{L}_ν^{LBG} are equal. We conclude that DLAs with [C II] 158 μm cooling characterised by $\ell_c > 10^{-27.1}$ ergs $\text{s}^{-1}\text{H}^{-1}$ contain centrally located LBGs, and that these values of ℓ_c are signatures of LBG activity. Furthermore, the cooling arises from CNM gas with a significant area covering factor. By contrast, DLAs with $\ell_c < 10^{-27.1}$ ergs $\text{s}^{-1}\text{H}^{-1}$ do not contain LBGs and in this case the gas is a WNM mainly heated by background radiation.

Acknowledgements

The author thanks E. Gawiser, J. Miralda-Escude, and J. X. Prochaska for valuable comments. This research was partially supported by NSF grant AST 03-07824.

References

- Bakes, E. L. O., Tielens, A. G. G. M., 1994, *ApJ*, 427, 822
 Bouche, N., Lowenthal, J. D., 2003, *ApJ*, 609, 513
 Bunker, A., *et al.*, 2004, private communication
 Chen, H.-W., Kennicutt, R. C., Rauch, M., 2005, *ApJ*, 620, 703
 Cooke, J., Wolfe, A. M., Prochaska, J. X., Gawiser, E., 2005, in preparation
 Gialvalisco, M., *et al.*, 2004a, *ApJ*, 620, L103
 Gialvalisco, M., *et al.*, 2004b, *ApJ*, 600, L93
 Haardt, F., Madau, P., 2004, private communication
 Kulkarni, V. P., *et al.*, 2001, *ApJ*, 536, 36
ibid., 2000, *ApJ*, 551, 37
 Miralda-Escude, J., 2005, *ApJ*, 620, 91
 Møller, P., Fynbo, J. P. U., Fall, S. M., 2004, *A&A*, 422, L33
 Møller, P., Warren, S. J., Fall, S. M., Fynbo, J. P. U., Jakobsen, P., 2002, *ApJ*, 574, 51
 Nagamine, K., Springel, V., Hernquist, L., 2004 *MNRAS*, 348, 421
 Prochaska, J. X., Wolfe, A. M., 1996, *ApJ*, 470, 403
 Schaye, J., 2001, *ApJ*, 559, L1
 Shapley, A. E., Steidel, C. C., Pettini, M., Adelberger, K. L., 2003, *ApJ*, 588, 65
 Steidel, C. C., Adelberger, K. L., Gialvalisco, M., Dickinson, M., Pettini, M., 1999, *ApJ*, 519, 1
 Viegas, S. M., 1995, *MNRAS*, 276, 268
 Weingartner, J. C., Draine, B. T., 2001, *ApJS*, 134, 263
 Wolfe, A. M., Gawiser, E., Prochaska, J. X., 2003, *ApJ*, 593, 235 (WGP03)
 Wolfe, A. M., Gawiser, E., Prochaska, J. X., 2005, *ARA&A*, 43, (WGP05)
 Wolfe, A. M., Howk, J. C., Gawiser, E., Prochaska, J. X., Lopez, S., 2004,
 Wolfe, A. M., Prochaska, J. X., Gawiser, E., 2004,
ApJ, 615, 625 (WHGPL04)
 Wolfire, M. G., McKee, C. F., Hollenbach, D., Tielens, A. G. G. M., 2003, *ApJ*, 587, 278
 Wright, E. L., *et al.*, 1991, *ApJ*, 381, 200